A route to chaos in the Boros–Moll map

Laura Gardini

Department of Economics, Society, Politics (DESP), University of Urbino, Italy
E-mail: laura.gardini@uniurb.it

Víctor Mañosa

Department of Mathematics, Universitat Politècnica de Catalunya, Spain
E-mail: victor.manosa@upc.edu

Iryna Sushko

Institute of Mathematics, National Academy of Sciences of Ukraine, Ukraine
E-mail: sushko@imath.kiev.ua

Abstract

The Boros-Moll map appears as a subsystem of a Landen transformation associated to certain rational integrals and its dynamics is related to the convergence of them. In the paper, we study the dynamics of a one-parameter family of maps which unfolds the Boros-Moll one, showing that the existence of an unbounded invariant chaotic region in the Boros-Moll map is a peculiar feature within the family. We relate this singularity with a specific property of the critical lines that occurs only for this special case. In particular, we explain how the unbounded chaotic region in the Boros-Moll map appears. Special attention is devoted to explain the main contact/homoclinic bifurcations that occur in the family. We also report some other bifurcation phenomena that appear in the considered unfolding.

1   Introduction

In this paper we study some dynamical properties of the one-parameter family of planar maps $G_h : \mathbb{R}^2 \to \mathbb{R}^2$ given by

$$G_h(x, y) := \left(\frac{h(x+y) + xy + 9}{(x+y+2)^{4/3}}, \frac{x+y+6}{(x+y+2)^{2/3}} \right). \tag{1}$$

For $h = 5$, the map G_5 appears as a subsystem on an uncoupled Landen transformation defined in $\mathbb{R}^5$ introduced by Boros and Moll in [3], see also [4]. Roughly speaking, given a definite integral depending on several parameters, a Landen transformation is a map on these parameters that leaves invariant the integral, see [20, p. 412] for a more precise definition, and [1] for a historical account of Landen transformations. Indeed, in the above references it is shown that the dynamical system defined by

$$\begin{cases} a_{n+1} = \dfrac{5a_n + 5b_n + a_n b_n + 9}{(a_n + b_n + 2)^{4/3}}, \quad b_{n+1} = \dfrac{a_n + b_n + 6}{(a_n + b_n + 2)^{2/3}}, \\[2ex] c_{n+1} = \dfrac{d_n + e_n + c_n}{(a_n + b_n + 2)^{2/3}}, \quad d_{n+1} = \dfrac{(b_n + 3)c_n + (a_n + 3)e_n + 2d_n}{a_n + b_n + 2}, \\[2ex] e_{n+1} = \dfrac{c_n + e_n}{(a_n + b_n + 2)^{1/3}}, \end{cases} \tag{2}$$

is a Landen transformation of the integral

$$I(a, b, c, d, e) = \int_0^\infty \frac{cx^4 + dx^2 + e}{x^6 + ax^4 + bx^2 + 1} \mathrm{d}x,$$

which means that $I(a_{n+1}, b_{n+1}, c_{n+1}, d_{n+1}, e_{n+1}) = I(a_n, b_n, c_n, d_n, e_n)$. The map G_5 is, therefore, the one associated with the subsystem of the denominator's parameters of the integral. This map has been

investigated from a dynamical view point by Chamberland and Moll in [5], proving that the set of values of the parameters for which the integral associated to the 5-dimensional Landen transformation converges, coincides with the basin of attraction of one of the fixed points of the map G_5.

The study of the global dynamics of map G_5 is a challenging task. The known facts can be summarized as follows: There is a connected open set which is the basin of attraction of the fixed point $(x, y) = (3, 3)$. Coexisting with this basin, it appears an invariant set with chaotic dynamics.[1] The boundary between these sets is given by one of the two connected components of an algebraic curve (given in Eq. (6), below) that is part, together with its preimages, of the stable set of a saddle point that is also contained in the curve.

In this work we consider the unfolding of G_5 given by the one-parameter family (1) and we describe the route that leads to the appearance of the chaotic set for $h = 5$. In particular we analyze the maps G_h for $h \geq 5$, say $h \in [5, 6]$, pursuing the appearance of areas with chaotic dynamics and their bifurcations, and showing that there is a repelling chaotic set for $h \gtrsim 5$. We relate the existence of the chaotic set for $h = 5$ with the merging of a part of the critical line with the mentioned algebraic curve.

The paper is structured as follows. Section 2 is devoted to study the two main final bifurcations that appear in the family: the one that leads to the appearance of an unbounded chaotic repellor that exists for all the values of the parameter $h \in (5, \tilde{h}]$, where $\tilde{h} \simeq 5.032$; and the final creation of the invariant unbounded chaotic set of G_5. These bifurcations are studied in Sections 2.4 and 2.5, respectively.

The previous subsections are devoted to explain some general issues of the family of maps G_h. In Section 2.1 we introduce the notation concerning the so called *critical lines*, which is one of the main tools in our analysis, and we recall some of the main features of the phase portrait of the Boros-Moll map. In Section 2.2 we prove the existence of three fixed points for all the values of the parameter h, and we determine the value h_{NS} at which a Neimark-Sacker bifurcation of one of the fixed points occurs, that starts the sequence of bifurcations studied in the paper (see Fig.2 and Fig.9). In Section 2.3 we show that the dynamics of the family of maps for values of h greater than h_{NS} is regular.

Section 3 is devoted to describe some sequences of bifurcations, the main ones that appear in the selected route to chaos in the Boros-Moll map, with special emphasis in the creation and contact bifurcations of chaotic areas, and homoclinic bifurcations related to snap-back repellors.

An Appendix is included with some considerations regarding the partition of the phase space in zones related to the number of rank-1 preimages of the family of maps.

2 General properties of map G_h and main final bifurcations

2.1 Structure of the phase space of G_5

As mentioned in the Introduction, our aim is to describe how the chaotic set existing for the map G_5 is created. In Fig.1 we recall the structure in the phase space.

The determinant of the Jacobian matrix of any map G_h is

$$\det(J(G_h)) = -\frac{1}{3} \frac{(x + y - 6)(x - y)}{(x + y + 2)^3} \tag{3}$$

and therefore, for any fixed $h \in \mathbb{R}$ the critical curve LC_{-1} of a map G_h, is given by the two straight lines

$$\begin{aligned} LC_{-1}^j &: y = x, \text{ and} \\ LC_{-1}^{jj} &: x + y - 6 = 0. \end{aligned} \tag{4}$$

Since LC_{-1}^j intersects the line (d)

$$(d) : x + y + 2 = 0, \tag{5}$$

where the denominator of the components of the map vanishes, at the point $(x, y) = (-1, -1)$, the image[2] of LC_{-1}^j consists of two unbounded arcs $LC = G_h(LC_{-1}^j) = LC^j \cup LC_r^j$ which, in the case $h = 5$, are the

---

[1]It cannot be called a chaotic attractor, since the closure of a generic trajectory looks like the full invariant set, and attracts no other point.

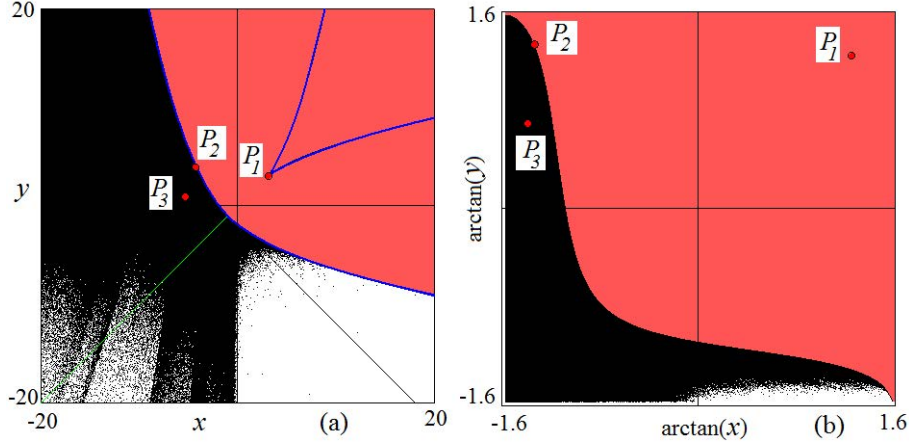[2]See [2] for details related to some properties of maps with a vanishing denominator.

Figure 1: Chaotic set (in black) and basin of attraction of $P_1 = (3, 3)$ (in red) for the Boros-Moll map G_5. In (a) in the phase plane (x, y). In (b) in the plane scaled as $(\arctan(x), \arctan(y))$.

two connected components of the resolvent curve given by

$$R(x, y) = -x^2 y^2 + 4 x^3 + 4 y^3 - 18 xy + 27 = 0. \tag{6}$$

For $h = 5$, the image of the portion of straight line LC^j_{-1} from infinity $(-\infty)$ to $(x, y) = (-1, -1)$ gives LC^j, the arc bounding the chaotic area in Fig.1, and belongs to the stable set of the saddle fixed point $P_2 \simeq (-4.20557, 3.95774)$, [12, Proposition 8]. The second branch of $G_5(LC^j_{-1})$, which is LC^j_r, is the image of the half line of LC^j_{-1} taken from $(-1, -1)$ to infinity $(+\infty)$, and it is also shown in Fig.1a. It includes the fixed point $P_1 = (3, 3)$ which is an attracting node whose basin is also bounded by LC^j. The third fixed point $P_3 \simeq (-5.30914, 0.83118)$ is an unstable focus belonging to the chaotic area. As noticed in [5], the fact that

$$R(G_5(x, y)) = \frac{(x - y)^2}{(x + y + 2)^4} R(x, y), \tag{7}$$

implies that the curve LC is invariant, i.e. $G_5^n(LC) = LC$ for any $n > 0$. By using the fact that LC^j is part of the stable set of the saddle point P_2 we also have that the arc LC^j is invariant. From this fact, and from the characterization of the basin of attraction of P_1 given in [5], the (seemingly chaotic) area bounded by the curve LC^j is also invariant. In fact, in [19] and [20, p. 442–444] it seems suggested that such invariant area is exactly a true chaotic area (with dense periodic points, which are all homoclinic), but this is still to be proved rigorously.

In order to understand the appearance of the chaotic area we consider the 2-parametric family of maps $G_{g,h} : \mathbb{R}^2 \to \mathbb{R}^2$ given by

$$G_{g,h}(x, y) := \left(\frac{gx + hy + xy + 9}{(x + y + 2)^{4/3}}, \frac{x + y + 6}{(x + y + 2)^{2/3}} \right),$$

for which a numerical exploration evidences that unfolding the Boros-Moll map there are maps with different qualitative behavior. Indeed, one can check that in the parameter plane (g, h) depicted in Fig. 2 there appear several regions indicating qualitative differences. The different colors in this figure represent regions in the parameter space related to the existence of attracting cycles of different periods. The yellow region in Fig. 2 represents the values of the parameters at which the dynamics is regular, namely there exist two attracting fixed points, P_1 in the positive side and P_3 in the negative side, whose basins of attraction are separated by the stable set of a saddle fixed point P_2. Differently, the brown region represents the values of the parameters at which the only attracting set is the positive fixed point P_1. The existence of these fixed points, as a function of the parameters, is commented below. The white points denote either existence of a cycle
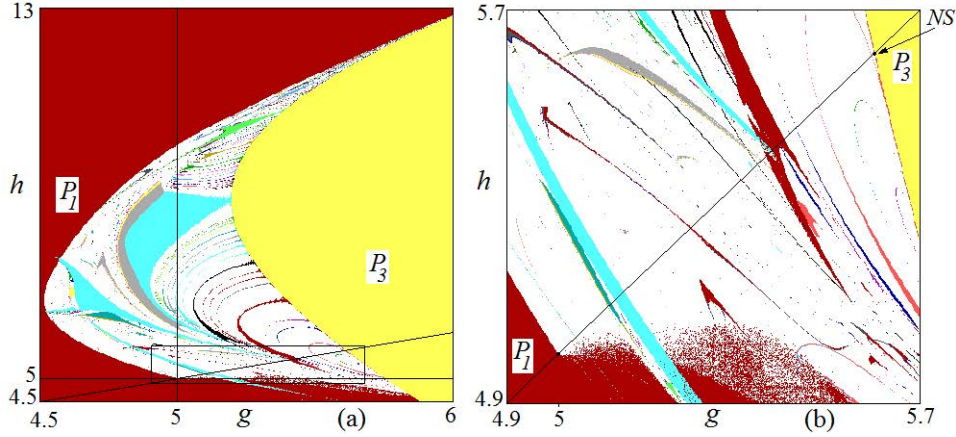
3

Figure 2: In (a) two-dimensional bifurcation diagram related to an i.c. close to the fixed point P_3. In (b) enlargement of the rectangle marked in (a).

of period higher than 45 or the existence of a chaotic attractor. Since the positive fixed point P_1 is always attracting, in all these regions the attractor P_1 coexists with some other attracting set. To simplify our analysis, which is oriented to understand the dynamics of the Boros-Moll map, we consider $g = h$, which gives the one-parametric family (1), and we will focus mainly in the interval $h \in [5, 6]$ of the parameter values. Thus, in the two-dimensional bifurcation diagram the straight line of equation $g = h$ represents the path that we shall follow in order to describe some of the bifurcations occurring from a regular regime existing for $h = 6$ to the chaotic one existing for $h = 5$. In fact, changing the parameter h along the path in Fig.2(b), decreasing h, the fixed point P_3 becomes an attracting focus and then it becomes a repelling focus via a Neimark-Sacker (NS from now on, for short) bifurcation, as commented below, giving rise to a sequence of bifurcations that we will summarize in its main features. Decreasing h we can comment the appearance/disappearance of attracting k-cycles for $k > 1$ of different periods or attracting closed invariant curves as well as the existence of chaotic attractors/repellors.

2.2 Fixed points of G_h and first Neimark-Sacker bifurcation

We notice that for any $h \in \mathbb{R}$, map G_h has exactly three different fixed points. In order to characterize the fixed points of map G_h, and following [5], we introduce the auxiliary variable $m^3 = x + y + 2$, so that the fixed points are characterized by

$$\begin{cases} c_1(x, y, m) & := m^3 - x - y - 2 = 0, \\ c_2(x, y, m) & := -xm^4 + xy + hx + hy + 9 = 0, \\ c_3(x, y, m) & := -ym^2 + x + y + 6 = 0. \end{cases} \tag{8}$$

Isolating x and y from the first and third equations we get:

$$x = \frac{m^5 - m^3 - 2m^2 - 4}{m^2} \text{ and } y = \frac{m^3 + 4}{m^2}. \tag{9}$$

Substituting these expressions in the second equation we obtain that the variable m must satisfy

$$c_4(m) = m^{11} - m^9 - 3m^8 - hm^7 - 3m^6 - 2m^5 + (2h - 9)m^4 + 8m^3 + 8m^2 + 16 = 0.$$

4

Observe that the term with highest degree in m of $c_4(m;h)$ does not vanish for any $h \in \mathbb{R}$, hence no root enters from infinity. On the other hand, the discriminant of c_4 is given by

$$
\begin{aligned}
\Delta_m(c_4(m;h)) = {} & 927712935936\, h^{14} - 29686813949952\, h^{13} + 211982405861376\, h^{12} \\
& + 2739735613145088\, h^{11} + 118044964423729152\, h^{10} - 1417849672260648960\, h^{9} \\
& - 3159536320125075456\, h^{8} - 89793115515877588992\, h^{7} + 2232890826264743510016\, h^{6} \\
& - 8668279665625562873856\, h^{5} + 39121043805342246371328\, h^{4} \\
& - 95808232773412768972800\, h^{3} + 82627725757886495509708 80\, h^{2} \\
& - 28385116733510952733900800\, h + 358440376501902152690565 12.
\end{aligned}
$$

By using the Sturm method we obtain that $\Delta_m(c_4(m)) > 0$ for all $h \in \mathbb{R}$, hence $c_4(m)$ has no multiple roots, so that no roots of $c_4(m)$ appear from $\mathbb{C}$ and there is no value of h such that the roots collide. Finally, using again the Sturm method we have that for $h = 5$, $c_4(m)$ has only three distinct real roots. Hence for all $h \in \mathbb{R}$ the polynomial $c_4(m)$ has three different real roots, which give rise to three different fixed points via Eq. (9).

As already noticed in [5] and recalled above, G_5 has the fixed points P_1, P_2 and P_3. Since the location of the fixed points vary continuously with the parameter h, we will denote the fixed points of the maps G_h as $P_1(h), P_2(h)$, and $P_3(h)$, not indicating the dependence on h when it is not necessary.

Since the fixed points P_1 and P_2 persist for $h \in [5,6]$ as an attracting node and a saddle, respectively, we are interested in the fixed point P_3 which may be attracting or repelling, as we have seen in Fig. 2. So we restrict the scope of our analysis to the proof of a NS bifurcation that occurs at $h \simeq 5.6105116077$. To find the parameter value where the NS bifurcation takes place we consider the equation $\det(DG_h(x,y)) = 1$, obtaining

$$
c_5(x,y,m) := 3\,(x+y+2)^3 + (x+y-6)\,(x-y) = 0.
$$

Using the polynomials c_1, c_2 and c_3 that characterize the fixed points, and taking successive resultants we get that if a NS bifurcation takes place then the parameter h must be a root of the polynomial

$$
\begin{aligned}
P_{NS}(h) = {} & 582371795533824h^{11} - 7007247733358592h^{10} + 413932755961774 08h^{9} \\
& - 557755817005154304h^{8} + 10296285821493313536h^{7} - 12903949700670 9473280h^{6} \\
& + 970090676944581427200h^{5} - 407249610096865443 8400h^{4} + 8531720267711624773632h^{3} \\
& - 7149146865159609778176h^{2} + 6956611779457796014080h - 20284715289100324700160
\end{aligned}
$$

By using the Sturm method we get that this polynomial has a unique real root in

$$
\left[\frac{808559935549815353}{144115188075855872}, \ \frac{404279967774907677}{72057594037927936} \right].
$$

Hence $h_{NS} \simeq 5.6105116077302352$. Now we check that the point $P_3(h)$ is a hyperbolic stable focus for $h \gtrsim h_{NS}$, a hyperbolic unstable one for $h \lesssim h_{NS}$ and non-hyperbolic for $h = h_{NS}$. In the next subsection we show that for $h > h_{NS}$ there is coexistence of the two attracting fixed points P_1 and P_3 and their basins of attraction are separated by the stable set of the saddle P_2.

2.3   Regular regime of the map G_h

As remarked above, for large values of h the dynamics of a map G_h is quite regular. In fact, the map has two attracting fixed points, P_1 and P_3. An example of the phase plane in such a situation is shown in Fig.3, for $h = 6$, where $P_1 \simeq (3.37349, 3.00069)$, $P_3 \simeq (-5.47727, 0.48573)$. In that figure the basin of attraction of the fixed point P_1 is shown in red, $\mathcal{B}(P_1)$, while that of P_3 is shown in yellow, $\mathcal{B}(P_3)$. The related basins of attraction are separated by the stable set of the saddle fixed point P_2.

The main difference with respect to the case $h = 5$ is that the main branch of the stable set of the saddle P_2 is not a critical curve and that the basin of the fixed point P_1 is not connected (for example, there are open sets of points with both negative coordinates that have a trajectory convergent to P_1). In Fig.3 it
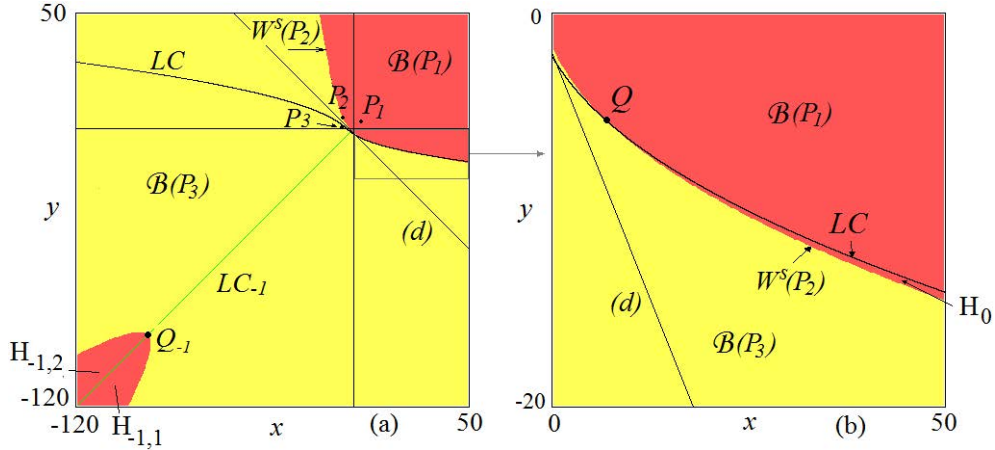
Figure 3: Basins of attraction of map G_h at $h = 6$.

is shown the straight line LC_{-1}^j up to the point $(-1, -1)$ and its image is the curve LC^j, shown in black, which intersects the line (d) (see (5)) in one point and also intersects the stable set $W^s(P_2)$ in one point Q (see the enlargement in Fig.3)[3]. The region denoted by H_0 in Fig.3, which is the portion of phase plane bounded above by the critical curve LC^j and below by the stable set $W^s(P_2)$ on the right side of the point Q, belonging to $\mathcal{B}(P_1)$, is responsible of further preimages belonging to the basin $\mathcal{B}(P_1)$.

In the Appendix, it is reported how the critical lines split the plane in different zones named Z_i where the sub-index i denotes the number of different rank-1 preimages. In what follows, we will use this notation. In fact, the arc of LC^j on the boundary of H_0 has two merging rank-1 preimages in the half line LC_{-1}^j up to the point Q_{-1}, while the arc of stable set $W^s(P_2)$ on the right side of the point Q has two distinct rank-1 preimages issuing from the point $Q_{-1} \in LC_{-1}^j$, one at the right side of LC_{-1} (on the boundary of the set $H_{-1,1}$) and the other at the left side (on the boundary of the set $H_{-1,2}$), forming the boundary of the set $H_{-1} = H_{-1,1} \cup H_{-1,2}$. Since H_{-1} belongs to the zone Z_2 whose points have two distinct rank-1 preimages, we have two more preimages of H_{-1} and so on, ad infinitum. Thus, the basin $\mathcal{B}(P_1)$ includes also the infinite sequence of preimages $\cup_{n \geq 1} G_h^{-n}(H_{-1})$ which consists of infinitely many portions of the plane (in fact, due to the properties of the regions Z_k described in Appendix, even if a preimage may happen to belong to Z_0 (so having no further preimages), another one above the diagonal exists, and thus it belongs to Z_k with $k \geq 2$.

2.4 Homoclinic bifurcation of P_2

The existence of non-connected regions of the phase plane belonging to the basin $\mathcal{B}(P_1)$ are relevant to prove that close to the value $h = 5$ a chaotic attractor becomes a chaotic repellor which persists for $h \in (5, \widetilde{h})$ for a certain value $\widetilde{h}$, although almost all the points of the phase plane have a trajectory convergent to the fixed point P_1. Similarly, a chaotic repellor exists for $h \in (5 - \varepsilon, 5)$ with $\varepsilon \gtrsim 0$, and almost all the points of the plane have a trajectory convergent to the fixed point P_1. Thus, the occurrence of an invariant set of positive measure (which seems chaotic) for $h = 5$ as shown in Fig.1 is a very peculiar phenomenon in the framework of dynamical systems theory. The peculiarity may be related to the basin $\mathcal{B}(P_1)$ which is an open simply connected set only for $h = 5$, and thus related to a peculiar behavior of the critical curves. In fact, for $h \in (5 - \varepsilon, \widetilde{h}) \setminus \{5\}$ the basin $\mathcal{B}(P_1)$ is an open set but not simply connected (while for $h \geq \widetilde{h}$ it is non connected).

We show that there exists a particular value $\widetilde{h} \simeq 5.032$ such that for $h > \widetilde{h}$, there exists an invariant unbounded absorbing region $\mathcal{A}$, which is bounded by segments of images of finite rank of a *generating segment* g belonging to the critical curve LC_{-1}^j for $x < -1$, that is, below the line (d) of vanishing denominator. For

---

[3]To simplify the notation, in the figures we write only LC in place of LC^j, since these are the only arcs of interest for the dynamics of the map, so there cannot be any confusion.

6

$h < \widetilde{h}$ such an invariant region does not exist[4]. Moreover, for $h > \widetilde{h}$ (resp. $h < \widetilde{h}$) the saddle fixed point P_2 is not homoclinic (resp. is homoclinic).

2.4.1 Situation before the contact and qualitative description of the contact bifurcation

For $h > \widetilde{h}$ (when the unbounded absorbing region $\mathcal{A}$ exists) the stable set of the saddle separates two basins of attraction: the basin $\mathcal{B}(P_1)$ of the attracting fixed point P_1 and the basin $\mathcal{B}(\mathcal{A})$ of the absorbing area $\mathcal{A}$ (inside which several attracting sets may exist). That is, the frontier of these two basins is that stable set: $W^s(P_2) = \partial\mathcal{B}(P_1) = \partial\mathcal{B}(\mathcal{A})$.
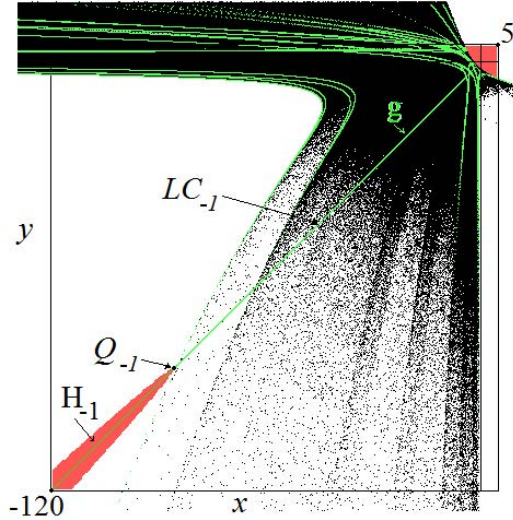
Figure 4: Phase portrait of map $G_{5.032}$. The white area belongs to the basin of the invariant chaotic area. The red area belongs to the basin $\mathcal{B}(P_1)$: In green, the images of the generating segment g of the critical line LC^j_{-1}. The region H_{-1}, which is part of the basin $\mathcal{B}(P_1)$, is close to contact with the chaotic area bounded the arcs given by the images of the generating segment.

In Fig.4 we illustrate the unbounded chaotic area at $h = 5.032$, whose boundary consists of a finite number of images of the generating segment g which is the arc of LC^j_{-1} belonging to the invariant area itself (see [18]). It can be seen that the boundary is very close to contact the point $Q_{-1} \in LC^j_{-1}$ on the boundary of the set H_{-1} which belongs to the basin $\mathcal{B}(P_1)$. Recall that this boundary belongs to the stable set of the saddle, $W^s(P_2)$, while the left branch of the unstable set of the saddle, $W^{u,l}(P_2)$, entering the chaotic area, is dense in that area (differently, the other branch $W^{u,r}(P_2)$ issuing from the saddle P_2 is a branch connecting the saddle with the attracting fixed point P_1). When such a contact occurs, say at $h = \widetilde{h}$, that is, when the boundary of H_{-1} has a contact with the critical curve bounding the chaotic area, then this contact leads (for $h < \widetilde{h}$) to the destruction of the invariant chaotic area and simultaneously to the appearance of homoclinic points of the saddle P_2 (but on the left side only). The role played by contact bifurcations of this kind have been described in several works (see e.g. [7] and [18]), see also the bifurcations called "crisis" in [13, 14].

The contact bifurcation occurring at $h = \widetilde{h}$ is qualitatively shown in Fig.5. The contact point between the region H_{-1} (whose boundary belongs to the stable set $W^s(P_2)$) and the chaotic area bounded by arcs of critical curves, is denoted by $p_k \in LC^j_k$ for a suitable integer k, and it is the image of a point $p_{-1} \in g \subset LC^j_{-1}$. If the area is truly chaotic then the closure of the unstable set $W^{u,l}(P_2)$ is exactly the chaotic area (i.e. $W^{u,l}(P_2)$ is dense in the area), which means that the arcs of critical curves are limit sets of the unstable set (arcs shown in blue in Fig.5). The image of p_k is the point $p_{k+1} \in LC^j_{k+1}$ belonging to the boundary of H_0 on the arc of the stable set $W^s(P_2)$, so that the same property holds for the forward images which

---

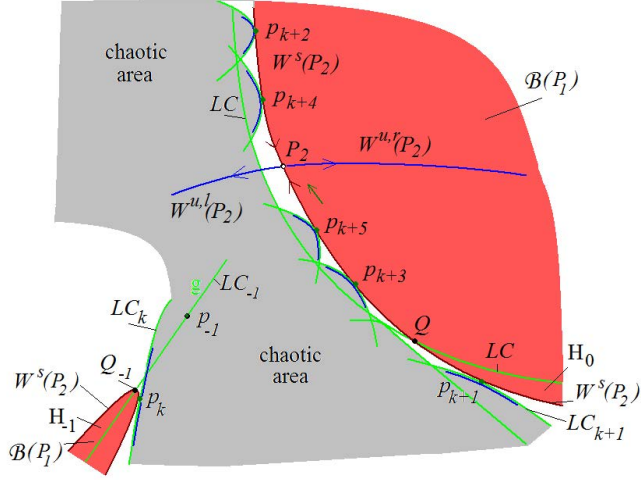[4]For $h = 5$ there exist an invariant area, but it is not absorbing.

Figure 5: Qualitative description of the contact bifurcation occurring at $h = \widetilde{h}$.

are converging to the saddle fixed point P_2: that is, they are contact points between critical arcs on the boundary of the invariant area $\mathcal{A}$ and the main branch of the stable set $W^s(P_2)$.

2.4.2 Situation after the contact bifurcation

For $h < \widetilde{h}$ when the critical curves intersect the regions H_{-1} and H_0 also the unstable set $W^{u,l}(P_2)$ is crossing these regions, and thus is crossing the stable set $W^s(P_2)$ leading to homoclinic points of the saddle, and since an invariant absorbing area no longer exists the generic trajectory converges to the attracting fixed point P_1.

Recall that for noninvertible maps we cannot refer to a general theorem stating that when a homoclinic orbit of a saddle cycle exists then close to the homoclinic orbit we can find an invariant set which is chaotic (in the sense of Devaney [6] and of Li and Yorke [15]), because the standard theorem holds for diffeomorphisms. However, also for endomorphisms (having not a unique inverse) it is possible to prove that following the homoclinic orbit in the proper way, with the suitable inverses applied to the homoclinic points, it is possible to show that a horseshoe can be rigorously defined, leading to the result. Examples can be found in [10] and [16].

Thus, for $5 < h < \widetilde{h}$ the chaotic attractor becomes a chaotic repellor, the only attracting set is the fixed point P_1, and its basin $\mathcal{B}(P_1)$ is almost the whole plane. The points of the plane on the left side of the main branch of the stable set of the saddle P_2 that are leaving that side converging to the attracting fixed point P_1 are doing so ultimately crossing through the regions called H_{-1} and H_0, where H_0 is always defined as above: it is the strip between the main branch of the stable set of P_2 and the arc of critical curve LC^j above it, which exists as long as $h > 5$ (as shown below). Notice that also the unstable set of the saddle P_2 for $5 < h < \widetilde{h}$ has points crossing through these regions. That is: arcs belonging to the unstable set $W^{u,l}(P_2)$ as well as arcs belonging to the critical lines LC_n^j for some $n > 1$ have points which cross through H_{-1} and H_0 and then converge to the attracting fixed point P_1.

2.5 Final bifurcation for $h = 5$. Role of the critical lines

At $h = 5$, the scene described in Section 2.4 is no longer possible because the strip H_0 reduces to the arc LC^j which merges with the main branch of the stable set of the saddle P_2, and thus the portion H_{-1} reduces to an arc of LC_{-1}^j. The portion of plane bounded by the arc of curve LC^j (belonging to the resolvent curve given in Eq.(6)) is invariant: it is the situation shown in Fig.1. Notice that the saddle P_2 is homoclinic, since the whole segment LC_{-1}^j and all its preimages belong to the stable set of P_2 and intersections between the stable and unstable sets are infinitely many, but only on the left side of the arc LC^j. This means that,

differently from the case for $5 < h < \widetilde{h}$, even if the saddle P_2 is homoclinic no one point belonging to the unstable set $W^{u,l}(P_2)$ can have a trajectory convergent to P_1 (since no one point can be mapped to the right side of LC^j) and similarly no point on the images of the critical line LC^j_{-1}, of any rank, can converge to P_1.

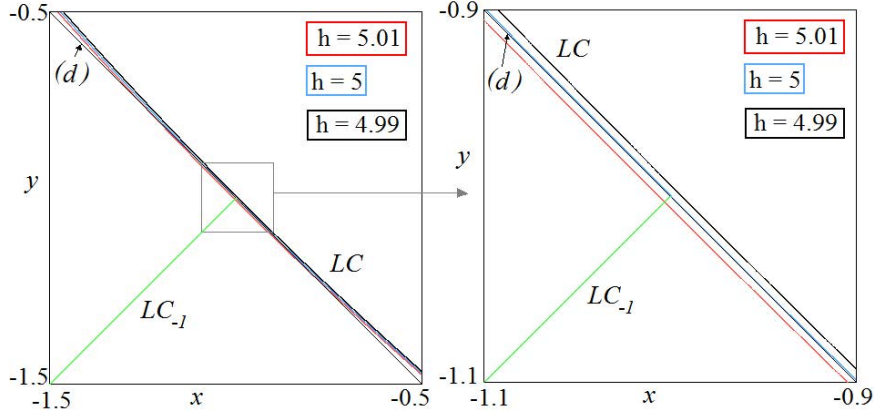So we have seen that for $5 \le h < \widetilde{h}$ the saddle P_2 is homoclinic only on the left side. The characteristic

Figure 6: Images of an arc of LC^j_{-1} for $x \le -1$ at $h = 5.01$, $h = 5$ and $h = 4.99$.

commented above associated with the Boros-Moll map at $h = 5$ may be related to the critical curves as follows. For $5 < h < \widetilde{h}$ the image of the critical curve LC^j_{-1} for $x \le -1$ is an unbounded branch LC^j which intersects the line of vanishing denominator (d) in two points, so that LC^j_1 consists in three unbounded components. In Fig.6 we show a portion of phase plane, an enlargement close to $(-1, -1)$ at $h = 5.01$, at this value of the parameter almost all the points have a trajectory converging to $P_1 \simeq (3.00375, 3.00000)$. At $h = 5$ the image of LC^j_{-1} for $x \le -1$ is the branch LC^j which merges with the main arc of the stable set of P_2, which is tangent (from above) to (d) in the point $(-1, -1)$, and it is invariant, so that $LC^j = LC^j_n$ for any $n \ge 1$. For $h < 5$ the image of LC^j_{-1} for $x \le -1$ is the branch LC^j completely above (d), and thus its points converge to the attracting fixed point P_1. Clearly, all the points in the strip H_0 between the main arc of the stable set of P_2 and the arc LC^j are also converging to the attracting fixed point P_1, and so do the points of its preimage belonging to a strip including LC^j_{-1} as well all the further preimages of any rank. For instance, at $h = 4.99$, a chaotic repellor still exists (since the fixed points P_2 and P_3 are homoclinic, as well as infinitely many repelling cycles exist and are homoclinic), and almost all the points are converging to $P_1 \simeq (2.99625, 3.00000)$.

For $h < 5$ not only the critical curves are on the right side of the main branch of the stable set of P_2, but also the unstable set $W^{u,l}(P_2)$ has again arcs going to the right side and converging to P_1.

In Fig.7 we illustrate an arc of LC^j_{-1} for $x \le -1$, LC^j in red and its first images, at $h = 5.01$, which are all on the left side of the curve LC^j, while at $h = 4.99$ the images are all on the right side to the LC^j (clearly for $h = 5$ this branch of LC^j is invariant).

The above study evidences that the arc LC^j is intersecting the main arc of the stable set $W^s(P_2)$ in one point Q as long as $h > 5$, they are merging when $h = 5$, and LC^j is above that stable set for $h < 5$.

3 Route to chaos

In order to describe the dynamics of map G_h (leading to the unbounded chaotic set shown in Fig.4) we account some of the phenomena that appear when the parameter h is decreased to $h = 5$ after the NS bifurcation of the fixed point P_3, that is, decreasing h from $h_{NS} \simeq 5.6105$. The NS bifurcation is of supercritical type, as can be seen from the attracting closed curve Γ which appears surrounding the repelling focus P_3, an example is illustrated in Fig.8a. The restriction of the map to the invariant curve in general leads either to an attracting cycle (when the rotation number is rational and the closed curve consists of a saddle-node connection) or to quasiperiodic orbits, dense in the closed curve (when the rotation number is irrational).
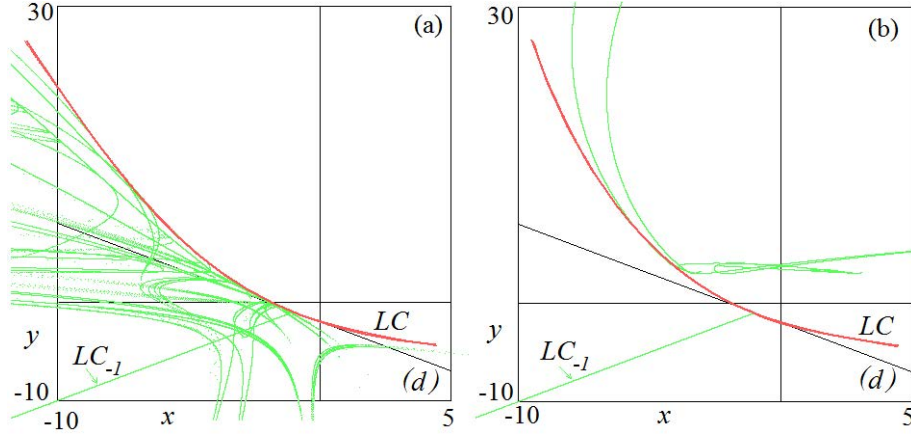
9

Figure 7: Critical curves LC_k^j for $1 \leq k \leq 4$ at $h = 5.01$ in (a), at $h = 4.99$ in (b).

It is worth noting that as long as the curve Γ is in a region without intersections with the critical curve LC_{-1}^j then all the points inside the area bounded by Γ cannot be mapped outside the area (i.e. the area bounded by Γ is invariant). At the same time, the points external to that area which are attracted from Γ have the trajectory completely outside Γ (i.e. the points are approaching the closed curve from outside). The dynamics in the phase plane change, as well as the global shape of the curve Γ, after a crossing of the critical curve LC_{-1}^j.
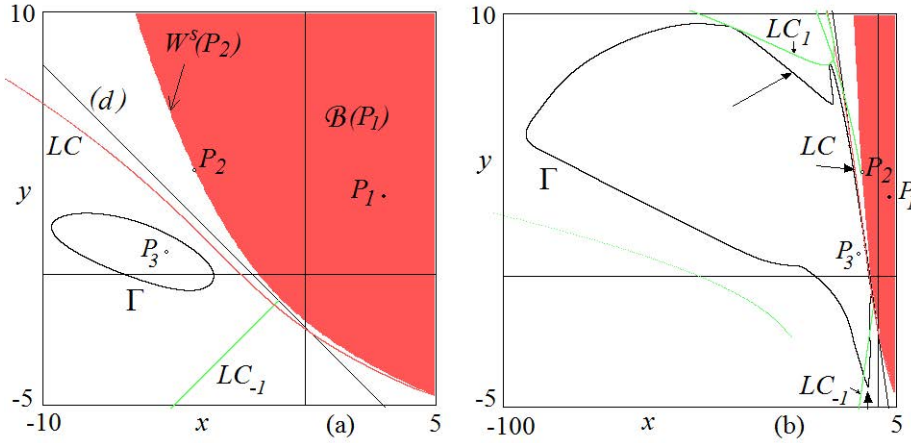
Figure 8: Bifurcation of the closed curve Γ. In (a) $h = 5.6$, smooth curve not intersecting LC_{-1}^j. In (b) $h = 5.44$, Γ intersects LC_{-1}^j.

Decreasing h a contact between Γ and LC_{-1}^j occurs at $h \simeq 5.506$, after which there is a portion of Γ which is below the critical curve and thus the portion of area bounded by Γ and crossing LC_{-1}^j is folded on LC^j so that Γ becomes tangent to LC^j in two points (the rank-1 images of the two intersection points $\Gamma \cap LC_{-1}^j$). And clearly the contacts between Γ and the critical curves LC_n^j persist for any n. In Fig.8b it is well evident the tangency between Γ and the critical curve LC_1^j.

This mechanism is a peculiar phenomenon related to noninvertibility (i.e. it cannot occur in maps with a unique inverse). It is related to the folding of the phase plane due to the critical curves, and breaks the invariance of the area bounded by the closed curve Γ. In fact, all the points in the area bounded by Γ and LC_{-1}^j are mapped outside Γ, between Γ and LC^j, and its further images between Γ and LC_1^j, and so on (see
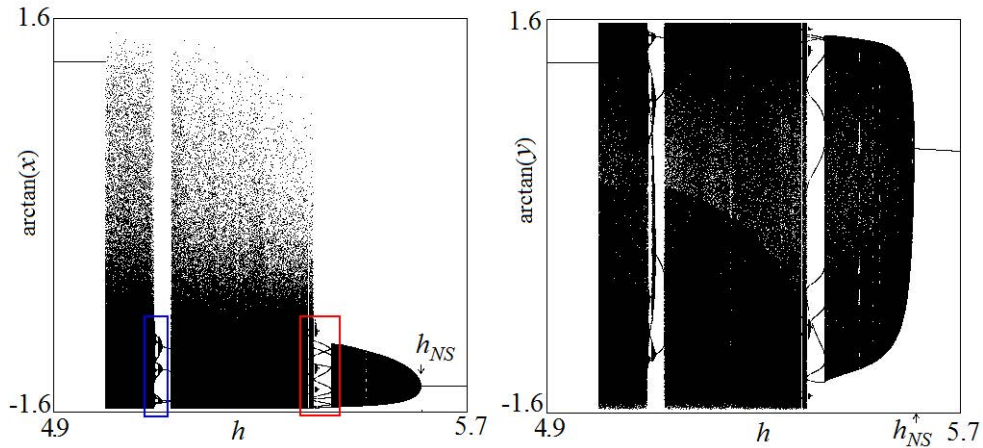
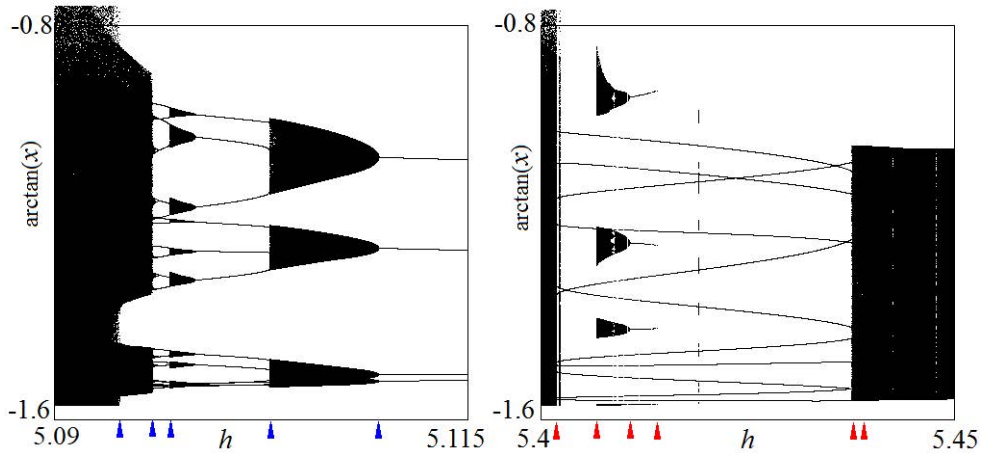Figure 9: One-dimensional bifurcations diagrams.

Figure 10: One-dimensional bifurcations diagrams. Enlargements of the rectangles shown in color in Fig.9a.

the related properties in [8] and [18]). In particular, this fact allows the existence of cycles of the map with periodic points both inside and outside the area bounded by the closed curve. We shall see an example in the next subsection.

Let us first illustrate a sequence of attractors and their bifurcations via one-dimensional bifurcation diagrams as a function of the parameter h. Since we know that unbounded attracting sets exist, in Fig.9 we show the scaled variable (as we have done in Fig.1b) to better emphasize when an attractor is unbounded. In Fig.9 it is evident the range in which decreasing h from h_{NS} the closed invariant curve Γ increases in size, since approaching the straight line (d) the shape becomes wider. In the same figure we see that there are two large windows associated with cycles and interesting dynamics, which are enlarged in Fig.10 and commented in the next subsections.

3.1 Bifurcations occurring in the first enlargement.

As noticed above, the oscillations on the closed curve Γ become pronounced as h is decreased. Moreover, other attracting sets appear by saddle-node bifurcation. An example is shown in Fig.11. At $h = 5.4379$ besides P_1 only the closed curve Γ is attracting, while at $h = 5.4378$ we can see that a pair of 11-cycles have

11

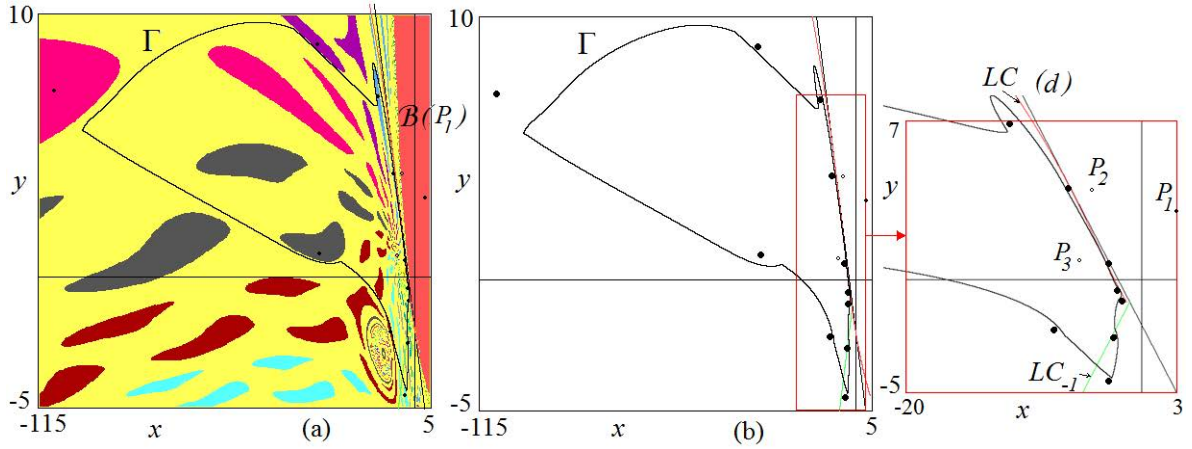appeared. One of them is attracting, while the other is a 11-cycle saddle whose stable set bounds the basin

Figure 11: Coexistence of the closed curve Γ and an attracting 11-cycle at $h = 5.4378$.

of attraction of the attracting 11-cycle, separating its basin from the basin of Γ. In Fig.11a we show in red (resp. yellow) the basin of P_1 (resp. the closed curve Γ) and we show with different colors the basins of the 11 fixed points of the 11-th iterate of the map G_h, to emphasize the shape of the basin of the attracting 11-cycle. In Fig.11b and related enlargement it can be seen that some points of the attracting 11-cycle are outside the closed curve Γ and part are inside. One more peculiarity related to the immediate basins of the 11 fixed points of map G_h^{11} is that the stable set of the 11 saddles (related to the 11-cycle saddle) leads to a closed curve, which is possible only in noninvertible maps, due to the crossing of the critical curves of the map (other examples and explanation of the mechanism can be found in [18]). From the same Fig.11 we can
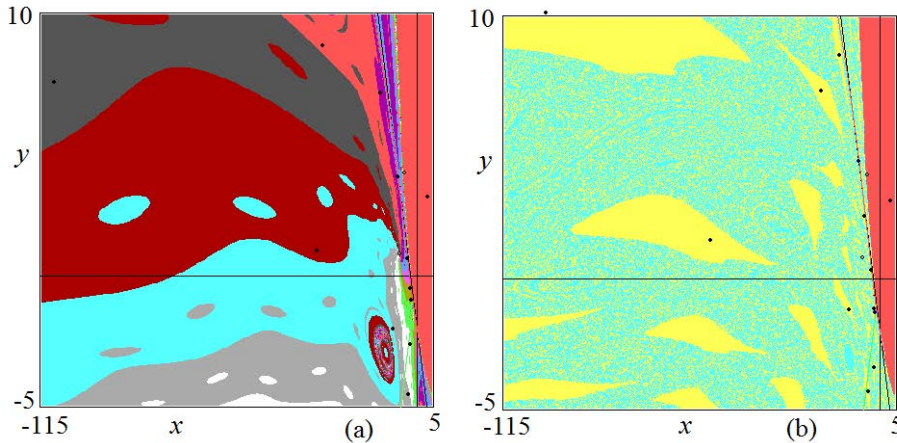

Figure 12: In (a) $h = 5.437$, attracting 11-cycle and its basin of attraction for the 11-th iterate of the map. In (b) $h = 5.412$, coexistence between the attracting 11-cycle and the attracting 4-cycle (in yellow and azure their respective basin of attraction).

see that the curve Γ is quite close to the stable set of the saddle 11-cycle on the boundary of the basin of attraction. A contact between these two invariant sets may lead to the disappearance of the closed curve Γ, and its transition to some repelling set. In any case, at $h = 5.437$ besides P_1 only the 11-cycle is attracting, and the stable set of the saddle 11-cycle has now a quite different shape, confirming the disappearance of the

12

closed invariant curve, as shown in Fig.12a, where the crossing of LC^j of the stable set of the saddle leads to the disconnected components evidenced in Fig.12a for the 11-th iterate of the map.

Decreasing h, one more saddle-node bifurcation occurs, now giving rise to a 4-cycle. As can be seen in Fig.10b this occurs at $h \simeq 5.4125$ leading to another coexistence of attracting sets on the left side of the main branch of the stable set of P_2. In Fig.12b at $h = 5.412$ besides P_1 (with basin in red) the basins of attraction of the 11-cycle (in yellow) and of the 4-cycle (in azure) are shown. The basins' structure of the two coexisting attractors is clearly fractal, which means that the saddle 11-cycle on the immediate basin of the 11-cycle is now homoclinic on one side (that external to the immediate basin which is clearly visible in yellow via bounded closed pieces). As evidenced in Fig.10b the attracting 4-cycle undergoes a supercritical NS
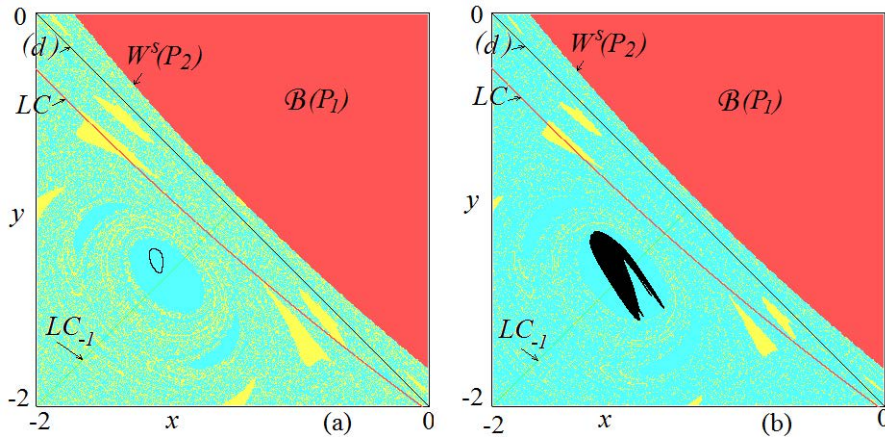

Figure 13: In (a) $h = 5.41$, NS bifurcation of the 4-cycle. In (b) $h = 5.40676$, chaotic piece showing that the 4-cycle is a snap-back repellor.

bifurcation at $h \simeq 5.411$ which leads to 4-cyclic closed invariant curves (see an example in the enlargement of Fig.13a at $h = 5.41$). The closed curves undergo bifurcations to annular chaotic regions and to 4-cyclic chaotic pieces (see the portion of phase plane in Fig.13b at $h = 5.40676$). This sequence, as described in [9] (see also [18]), leads to the homoclinic bifurcation of the expanding 4-cycle, repelling focus, which becomes a snap-back repellor (following Marotto [17]). The chaotic piece of the 4-cyclic set shown in Fig.13b is very close to the boundary of its basin of attraction, and a contact with the basin leads to the disappearance of the 4-cyclic chaotic pieces, which become a chaotic repellor. Already at $h = 5.40675$ a chaotic transient can be observed and the only attractor left on the left side of the main arc of the stable set $W^s(P_2)$ is the 11-cycle (with a chaotic repellor on its basin boundary).

The attracting 11-cycle disappears with the companion saddle cycle in a (reversed) saddle-node bifurcation. After this saddle-node bifurcation we cannot observe a simple attracting cycle, but a closed invariant absorbing area exists, inside which the dynamics seem chaotic. At $h = 5.4$ the area shown in Fig.14a intersects the critical line LC^j_{-1} in two segments, forming together the generating segments whose images bound the absorbing area via segments of critical curves. The area is unbounded as in fact the image of the shortest segment (evidenced in dark green in Fig.14a) is mapped in an arc of LC^j which crosses the line (d) of vanishing denominator (evidenced with a dark green arrow in Fig.14a), thus its image consists in two unbounded arcs of LC^j_1 on the boundary of the area. In Fig.14b it is shown a wider portion of phase space and in green the arcs of critical curves on the boundary of the invariant area, while in Fig.14c it is represented the unbounded attracting area in the whole plane, related to the scaled variables.

3.2 Bifurcations occurring in the second enlargement.

In the previous subsection we have described a few bifurcations which occur decreasing h and evidenced in Fig.10b, leading to an unbounded invariant absorbing area, with complex dynamics. Clearly, inside this invariant area it is possible that stable cycles of high period exist, not detectable in our numerical simulations.
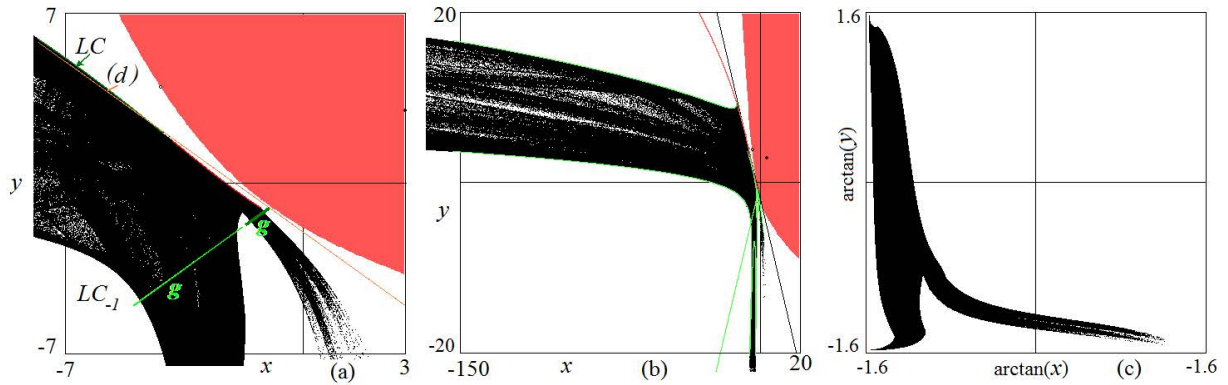
Figure 14: Unbounded absorbing area, with chaotic dynamics, at $h = 5.4$. In (a) the generating segments on LC_{-1}^{j} are evidenced. In (b) the attracting set is shown in a larger portion of the phase plane. In (c) the attracting set is shown the plane scaled as $(\arctan(x), \arctan(y))$.

However, cycles with homoclinic orbits also exist, both saddles and expanding cycles, as the 4-cycle described above which is a snap-back repellor (in fact, although an invariant 4-cyclic attracting chaotic area no longer exists, as evidenced by the complex dynamics, the homoclinic 4-cycle still exists). From Fig.9 we can see that the unbounded invariant absorbing area persists for a wide interval of values for the parameter h, and the appearance of an attracting 4-cycle leads to another window with interesting dynamics, enlarged in Fig.10a. The pair of 4-cycles appears by saddle-node bifurcation inside the invariant absorbing area.

In Fig.15a (at $h = 5.128$) we show the unbounded invariant area confined by portions of critical curves, and the generating segment is now a wider connected segment of LC_{-1}^{j}, in red are indicated the points where a pair of 4-cycles is going to appear. In Fig.15b (at $h = 5.127$) an attracting 4-cycle exists inside the invariant area, and its basin of attraction is evidenced with respect to the 4 points (in black) which are fixed for the 4-th iterate of the map G_h. The complex structure of the basins evidences a chaotic repellor on the basin boundary, while the immediate basins are (as in previous examples) bounded by the stable set of the saddle 4-cycle forming closed curves, denoting intersection with the critical curves. From Fig.10a we can see that
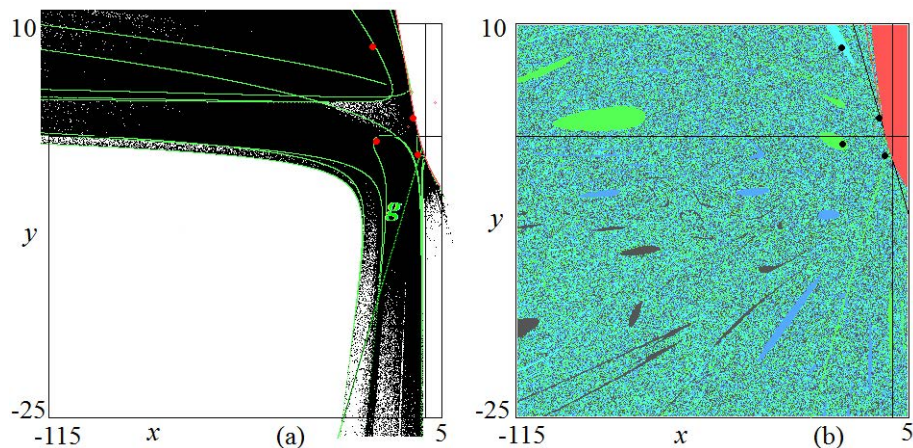

Figure 15: Appearance of an attracting 4-cycle. In (a) at $h = 5.128$ the cycles do not exsist. In (b) at $h = 5.127$ a pair of 4-cycles exist inside the unbounded invariant area.

the 4-cycle undergoes a NS bifurcation (at $h \simeq 5.11$), leading to 4-cyclic closed invariant curves which, from

14

smooth (for h close to the NS bifurcation) become nonsmooth after the crossing of the critical line LC^j_{-1}. We also see in Fig.10a that an attracting 12-cycle appears, which is related to the closed curves. In fact, at $h \simeq 5.10299$ the attracting set is no longer a smooth curve, since it is an invariant set with self intersections, as reported in Fig.16 (for the mechanism leading to the formation of loops and self intersections in closed curves see [8] and [18]).
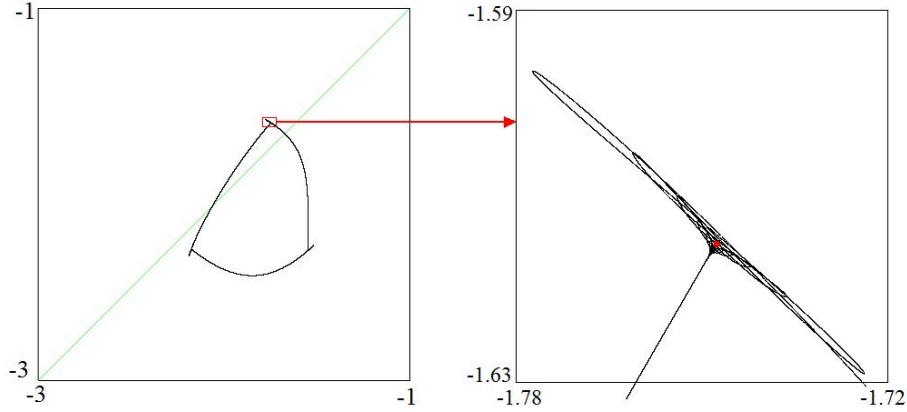

Figure 16: Enlargement showing one piece of the 4-cyclic invariant set at $h = 5.10299$ and appearance of the 12-cycle at $h = 5.10298$ represented by the red point in the further enlargement.

From Fig.10a we also see that, in its turn, the attracting 12-cycle undergoes a NS bifurcation, and after a sequence of bifurcations 12-cyclic chaotic pieces are created (see Fig.17a at $h = 5.097$). Other bifurcations are illustrated in Fig.17b at $h = 5.096$ (enlarged portion of phase plane, evidencing one piece of the 12-cyclic set). This, in its turn, is followed by a contact bifurcation at $h = 5.095$, leading to an expansion of the invariant absorbing area with chaotic dynamics which has now 4-cyclic chaotic pieces, one of them shown in Fig.17c. This also denotes that the repelling 4-cycle inside that area is now homoclinic, i.e. a snap-back repellor.

It is worth noting that all these attracting sets belong to the unbounded invariant absorbing area, generated by the segment as shown in Fig.15a. However, inside this region, we can find other invariant absorbing areas as the 4-cyclic areas which are all bounded by few images of the generating segment intersecting LC^j_{-1} and shown in Fig.17c. The 4-cyclic chaotic areas are shown at a lower value of h in Fig.18a, together with
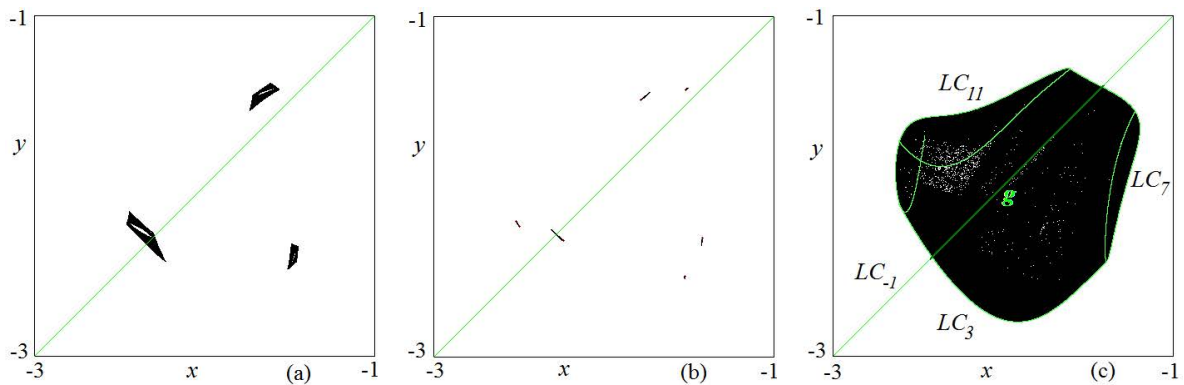

Figure 17: Enlargements showing a part of a chaotic attractor. Three pieces of an attractor of 12 connected components for $h = 5.097$ in (a); six pieces belonging to an invariant set of 24 connected components for $h = 5.096$ in (b); and one of 4 connected components for $h = 5.095$ in (c).

15

the related four basins of attraction for the 4-th iterate of the map. Besides a fractal structure with a chaotic repellor on the boundary, this figure shows that the areas are very close to the boundary of their immediate basins, denoting that the parameter is very close to a contact bifurcation value, leading to the disappearance of the 4-cyclic areas, and the appearance of a unique unbounded absorbing area inside which the dynamics seem chaotic, see Fig.18b.
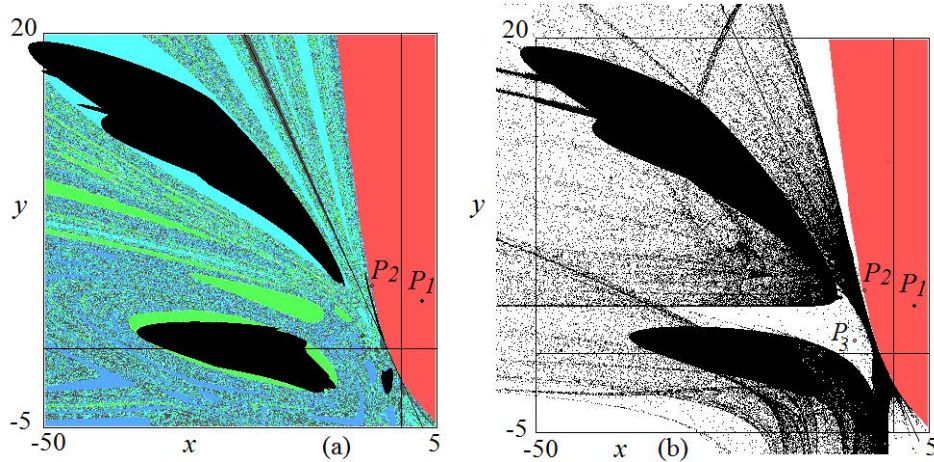

Figure 18: Contact bifurcation leading to expansion of the invariant area. In (a) $h = 5.09397$ 4-cyclic absorbing areas exist. In (b) $h = 5.09396$ the attracting set is an unbounded absorbing area.

The unbounded absorbing area previously obtained, persists for lower values of h, as shown in Fig.9, up to the bifurcation described in Sec.2.4.1 occurring at $h = \widetilde{h}$. Decreasing h up to the final bifurcation, it seems that the dynamics inside the unbounded absorbing area become more complex. That is, more cycles appear and undergo homoclinic bifurcations. For example the fixed point P_3 which is a repelling focus may become a snap-back repellor. From Fig.18b it is not clear whether it is homoclinic or not. However, we have evidence of this, at the same value $h = 5.09396$ used in Fig.18b.
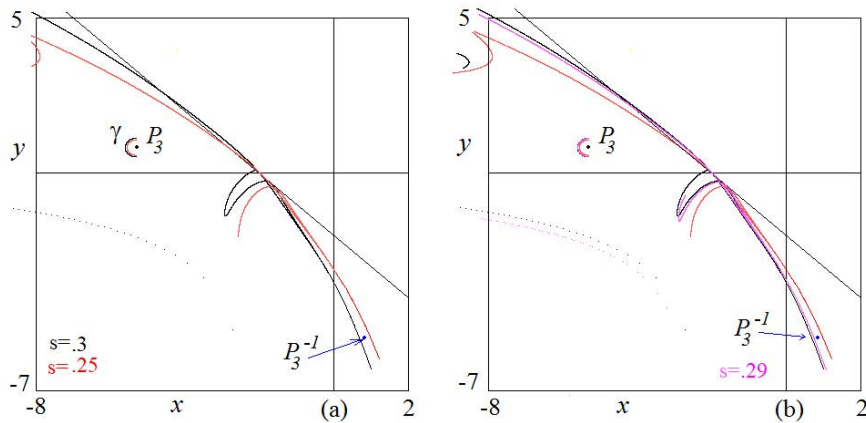

Figure 19: Images $G_{h^*}^{21}(\gamma)$ at $h^* = 5.09396$ of different arcs γ close to P_3 corresponding to different values of the radius s. In (a) two different arcs are shown. In (b) a third arc is added to the two shown in (a). The values of s are given in the text.

In fact, let us consider the fixed point P_3 and its rank-1 preimage different from itself, P_3^{-1}, which is the point symmetric to P_3 with respect to the main diagonal. In order to show that P_3 is a snap-back repellor

16

it is enough to show that there is a point q_0 in a neighborhood of P_3 which is mapped into P_3 in a finite number of iterations, say $G_h^m(q_0) = P_3$, and such that the local inverse which satisfies $G_h^{-1}(P_3) = P_3$ (which is a contraction), leads to $\lim_{n\to\infty} G_h^{-n}(q_0) = P_3$.

Let us consider an arc γ in such a neighborhood of P_3 (i.e. such that the preimages of its points by the local inverse G_h^{-1} converge to P_3), given by a half circle of equation

$$(x - x(P_3))^2 + (y - y(P_3))^2 = s^2$$

with the radius s sufficiently small. In Fig.19a we show such an arc γ in black corresponding to the radius $s = 0.3$, and the image $G_{h^*}^{21}(\gamma)$ (with $h^* = 5.09396$ as used in Fig.18b) in black which is close to the preimage P_3^{-1}, below it. Differently an arc γ in red corresponding to the radius $s = 0.25$, has the image $G_{h^*}^{21}(\gamma)$ in red which is close to the preimage P_3^{-1}, but above it. This means that there exists a value $s^* \in (0.25, 0.3)$ such that the related arc γ^* has the image $G_{h^*}^{21}(\gamma^*)$ which crosses through P_3^{-1}. This implies the existence of a point $q_0 \in \gamma^*$ such that $G_{h^*}^{22}(q_0) = P_3$.

As an example, considering $s = 0.29$ in Fig.19b we show in pink the related arc γ and, also in pink, the image $G_{h^*}^{21}(\gamma)$ which is above the black arc and closer to P_3^{-1}.

A similar construction can be used also at any smaller value of h (in particular also at $h = 5$ or smaller), showing that P_3 persists in being a snap-back repellor.

4   Conclusions

We have considered a one-parameter family of maps which unfolds a Landen-type map obtained by Boros and Moll, and we have described the main bifurcations that appear in the route towards the parameter value that corresponds to this map. We have focused on those homoclinic and contact bifurcations that can give information about the unbounded invariant chaotic region that appear in the Boros-Moll map. Our study confirms that the dynamics of this map is singular in the considered family, and we give evidences that this singularity is related with a specific property of the critical lines: the fact that one of the critical lines merges with one separatrix of the saddle point only for the parameter value corresponding with the map introduced by Boros and Moll.

Acknowledgements

References

[1] G. Almkvist, B. Gert. *Gauss, Landen, Ramanujan, the arithmetic-geometric mean, ellipses, π, and the Ladies diary*. Amer. Math. Monthly 95 (1988), 585–608.

[2] G.I. Bischi, L. Gardini, C. Mira. *Maps with denominator. Part 1: some generic properties*. Int. J. Bifurcation & Chaos 9 (1999), 119–153.

[3] G. Boros, V. H. Moll. *A rational Landen transformation. The case of degree six*. In M. Knopp et al. eds, "Analysis, Geometry, Number Theory: The Mathematics of Leon Ehrenpreis", Contemporary Mathematics 251. AMS, Providence RI 2000, 83–91.

[4] G. Boros, V. H. Moll. *Landen transformations and the integration of rational functions*. Mathematics of Computation 71 (2001), 649–668.

[5] M. Chamberland, V. H. Moll. *Dynamics of the degree six Landen transformation*. Discrete and Continuous Dynamical Systems A 15 (2006), 905–919.

[6] R. Devaney. "An introduction to chaotic dynamical systems", 2nd ed. Westview Press, Boulder CO 2003.

[7] D. Fournier-Prunaret, C. Mira, L. Gardini. *Some contact bifurcations in two-dimensional examples*. In "Grazer Mathematishe Berichte" (special issue Proceedings ECIT94) (1997), 77–96.

[8] C.F. Frouzakis, L. Gardini, Y.G. Kevrekidis, G. Millerioux, C. Mira. *On some properties of invariant sets of two-dimensional noninvertible maps*. Int. J. Bifurcation & Chaos 7 (1997), 1167–1194.

[9] L. Gardini. *Homoclinic bifurcations in n-dimensional endomorphisms, due to expanding periodic points* Nonlinear Analysis: Theory, Methods & Applications 23 (1994), 1039–1089.

[10] L. Gardini. *Homoclinic orbits of saddles in two-dimensional endomorphisms* In W. Förg-Rob et al. (editors) "Iteration Theory. Proceedings of the European Conference". World Scientific, Singapore 1996.

[11] L. Gardini, I. Sushko, V. Avrutin, M. Schanz. *Critical homoclinic orbits lead to snap-back repellers*. Chaos, Solitons & Fractals 44 (2011), 433–449.

[12] A. Gasull, M. Llorens, V. Mañosa. *Periodic points of a Landen transformation*. Preprint, arXiv:1801.04195 [math.DS]

[13] C. Grebogi, E. Ott, J. A. Yorke. *Crisis: sudden changes in chaotic attractors and transient chaos*. Physica D 7 (1983), 181–200

[14] C. Grebogi, E. Ott, F. Romeiras, J. A. Yorke. *Critical exponents for crisis-induced intermittency*. Physical Review A 36, 11 (1987), 5365–5380.

[15] T. Li, J.A. Yorke. *Period three implies chaos*. Amer. Math. Month. 82 (1975) 985–992.

[16] Y. Maistrenko, I. Sushko, L. Gardini. *About two mechanisms of reunion of chaotic attractors*. Chaos, Solitons & Fractals 9 (1998), 1373–1390.

[17] F. R. Marotto. *Snap-back repellers imply chaos in $\mathbb{R}^n$*. J. Math. Anal. Appl. 63 (1978) 199–223.

[18] C. Mira, L. Gardini, A. Barugola, J.C. Cathala. "Chaotic Dynamics in Two-Dimensional Noninvertible Maps", World Scientific, Nonlinear Sciences, Series A, Singapore 1996.

[19] V. H. Moll. *The evaluation of integrals: a personal story*. Notices Amer. Math. Soc. 49 (2002), 311–317

[20] V. H. Moll. "Numbers and functions. From a classical-experimental mathematician's point of view". Student Mathematical Library, 65. American Mathematical Society, Providence RI 2012.

5 Appendix

The map G_h has a non unique inverse, and the number of distinct rank-1 preimages of a point (x, y) differs depending on the region of the phase plane which the point (x, y) belongs to. These regions, or zones Z_i (related to i distinct preimages of rank-1) following the notation introduced in [18], are usually bounded by critical curves LC of the map, which are the images of curves of merging preimages, denoted LC_{-1}, which belong to the set where the Jacobian determinant of the map vanishes.

In our case, the Jacobian determinant vanishes either at the points LC_{-1}^j (defined by $y = x$) or the points in LC_{-1}^{jj} (defined by $x + y - 6 = 0$), see Eqs. (3) and (4).

Since LC_{-1}^j intersects (d), its image LC^j consists of two unbounded curves of the plane, $LC_l^j \cup LC_r^j$ (notice that if an arc γ crosses the line (d), where the denominator vanishes in a point in which the numerators of the components of the map do not vanish, which is always the case for the considered map, then its image $G_h(\gamma)$ consists of two unbounded arcs).
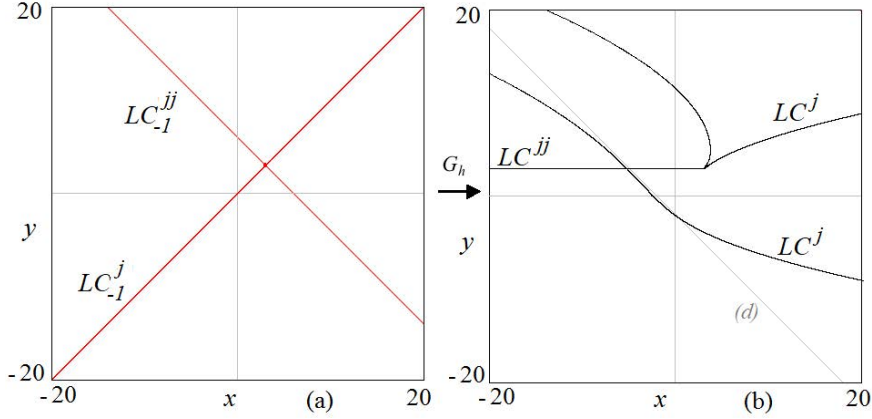
Figure 20: Critical curves for the map G_h at $h = 5.5$. In (a) LC_{-1}; in (b) LC.

The curve LC_{-1}^{jj} does not intersects (d), its image $LC^{jj} = G_h(LC_{-1}^{jj})$ consists of a single arc, and it is easy to see that it is a segment of straight line $y = 3$ (up to $x = 3$). Indeed, by setting $x_n = t$ and $y_n = -t+6$ (a point on LC_{-1}^{jj}), and taking $(x_{n+1}, y_{n+1}) = G_h(x_n, y_n)$ we get $x_{n+1} = (6t - t^2 + 39)/16$ (which takes its maximum value in $x = 3$) and $y_{n+1} = 3$, that is, the image of the line LC_{-1}^{jj} is folded on the half-line $y = 3$, as t increases from $-\infty$ to $+\infty$ and $x = t = 3$ is the folding point. In Fig.20 the critical curves for $h = 5.5$ are displayed.

In summary, the components of the critical curve $LC = LC^j \cup LC_r^j \cup LC^{jj}$ split the plane in 5 distinct open regions. We can figure out the number of preimages by considering a sort of "folding of the plane", as qualitatively shown in Fig.21. By computing how many preimages have *a particular point* in each of these regions, we obtain the different zones Z_i. In Fig.21 they are displayed for the particular case $h = 5.5$. Notice also that a point belonging to LC has two merging rank-1 preimages in a point belonging to LC_{-1}. For each point in a zone Z_i it is also possible to show where the preimages are located (on opposite side with respect to the related branch of LC_{-1}).

We report how to obtain the number of preimages in each of the zones limited by the curves LC. We fix a point (u, v) and we set $G_h(x, y) = (u, v)$. By introducing the notation $z = x + y + 2$ and from the equation of the second component of the map, we have that $vz^{2/3} = z + 4$, hence

$$v^3 = (z + 4)^3/z^2 \ . \tag{10}$$

By studying the function $f(z) = (z + 4)^3/z^2$ we easily get that for $v > 3$ there are three solutions of Eq. (10) (one negative and two positive); for $v = 3$ there is one negative solution and two merging solutions given by $z = 8$; and for $-\infty < v < 3$ there is only one negative solution.

Introducing the notation $P = xy$ and $S = x + y$, and by using the equation of the first component, we obtain that given (u, v) and a value of z satisfying Eq. (10), there is a unique value for P and S given by

$$P = u(z^4)^{1/3} - h(z - 2) - 9 \ \text{and} \ S = z - 2 \ .$$

Since any preimage (x, y) associated to (u, v) satisfies $y^2 - Sy + P = 0$ and $x = S - y$, we have

$$x = \frac{S \pm \sqrt{S^2 - 4P}}{2} \ \text{and} \ y = \frac{S \mp \sqrt{S^2 - 4P}}{2} \ .$$

The final number of preimages depends on the sign of $S^2 - 4P$.

For the original Boros-Moll map, the case $h = 5$, the curve LC^j belongs to the curve $R(x, y) = -x^2y^2 + 4x^3 + 4y^3 - 18xy + 27 = 0$, it is part of the stable set of the saddle P_2, and the zones Z_i are displayed in Figure 22.
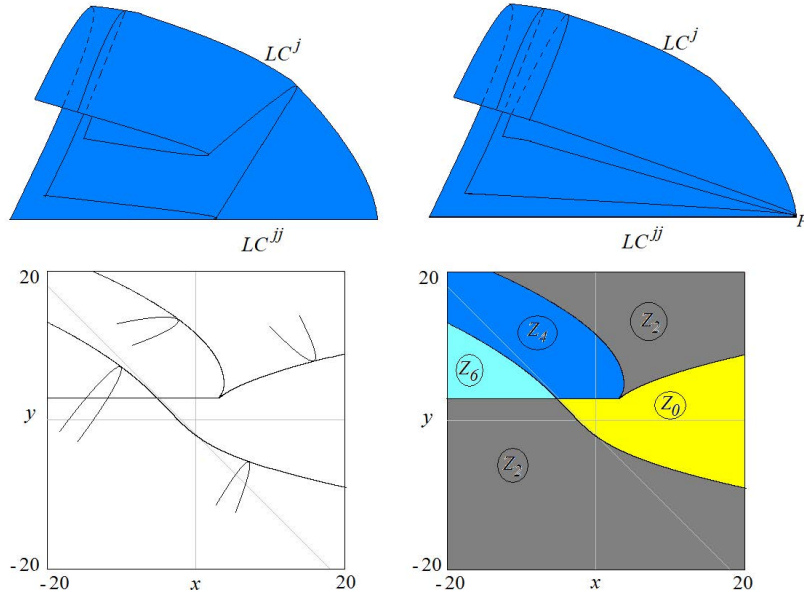
Figure 21: Qualitative shape of the foliation of the plane. Critical curves and Zones Z_i for the map G_h at $h = 5.5$.
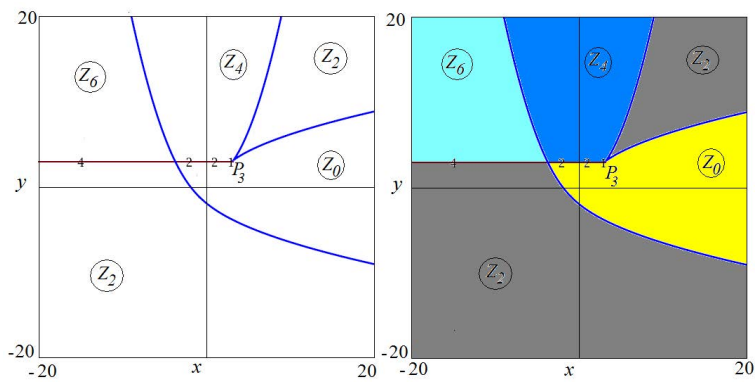

Figure 22: Critical curves and Zones for the Boros-Moll map ($h = 5$).